Desalination 280 (2011) 403–411

Contents lists available at ScienceDirect

Desalination

journal homepage: www.elsevier.com/locate/desal

An analytical model for spiral wound reverse osmosis membrane modules: Part I — Model development and parameter estimation

S. Sundaramoorthy [a,*], G. Srinivasan [a], D.V.R. Murthy [b,1]

[a] Department of Chemical Engineering, Pondicherry Engineering College, Pondicherry, 605014, India
[b] Department of Chemical Engineering, National Institute of Technology, Karnataka, Surathkal, 575025, India

ARTICLE INFO

Article history:
Received 24 November 2010
Received in revised form 15 March 2011
Accepted 16 March 2011
Available online 12 April 2011

Keywords:
Reverse Osmosis
Spiral wound module
Analytical model
Parameter estimation

ABSTRACT

A mathematical model for spiral wound Reverse Osmosis membrane module is presented in this work. The model incorporates spatial variations of pressure, flow and solute concentration in the feed channel and uniform conditions of pressure in the permeate channel. Assuming solution–diffusion model to be valid, explicit analytical equations were derived for spatial variations of pressure, flow, solvent flux and solute concentration on the feed channel side of the module. Analytical procedures for estimation of model parameters were presented. Graphical linear fit methods were developed for estimation of parameters Aw (solvent transport coefficient), Bs (solute transport coefficient) and b (feed channel friction parameter). The mass transfer coefficient k was assumed to vary along the length of the feed channel with varying conditions of flow, solute concentration and pressure. Explicit analytical equations for estimation of mass transfer coefficient were presented. In this paper (Part I), theoretical studies on development of mathematical model and methods for estimation of model parameters are presented.
In Part II of this paper series [1], Studies on validation of this model with experimental data are presented. The studies cover experimental work on a spiral wound RO module with an organic compound namely chlorophenol as a solute.

1. Introduction

Application of Reverse Osmosis (RO) membranes in the treatment of wastewater has grown rapidly over the past 30 years [2–6]. This has resulted in a global rise in the market for RO membrane technology in water and wastewater treatment and an increased interest in the development of cost effective design strategies that are needed for the optimal performance of RO systems. Development of appropriate mathematical models that adequately describe the performance of RO systems is very crucial for the optimal economic design of RO processes. More specifically, the models that can predict the performance of the RO systems under various operating conditions are essential for the economic planning and design of these systems for the treatment of waste water.

Industrial RO units are commonly available in three basic modular designs, namely plate and frame module, hollow-fiber module and spiral wound module [7–9]. Of these three modular designs, the spiral wound module is widely used due to high packaging density, moderate fouling resistance and lower capital and operating costs. In this work, development of mathematical models applicable to spiral wound RO modules is considered.

Any model that describes the behavior of complete spiral wound RO module requires three sub-models: one which describes the flow on the feed side of the module, the second one which describes the flow on the permeate side of the module and the third one which characterizes the separative properties of the membrane. Separative properties of the membrane are characterized by certain parameters that describe the relative transport of solute and solvent through membranes. Although there is a substantial amount of research work reported in the literature on the modeling of separative properties of the RO membranes, only a few models describing the performance of complete RO module have been developed.

More recently, Marriot et al., [10] have reported a general approach for modeling membrane modules in which they presented model equations that are applicable to both hollow fiber and spiral wound modules. Models for describing the performance of membrane modules are broadly classified as '*Approximate Analytical Models*' that typically assume average conditions on either side of the membrane and '*Rigorous Numerical Models*' that account for spatial variations in fluid properties throughout the module. *Analytical Models* are useful for simple design calculations, where as *Numerical Models* are used for more accurate simulation studies.

K.K. Sirkar et al., [11] have developed simple analytical design equations to calculate channel length and average permeate concentration

* Corresponding author. Tel.: +91 9444290056; fax: +91 413 2655101.
E-mail addresses: ssm_pec@yahoo.com (S. Sundaramoorthy), seenu_pec@yahoo.com (G. Srinivasan), dvrmvzm@gmail.com (D.V.R. Murthy).
[1] Tel.: +91 824 2474039; fax: +91 824 2474033.

0011-9164/$ – see front matter © 2011 Elsevier B.V. All rights reserved.
doi:10.1016/j.desal.2011.03.047

for spiral wound RO modules. In this work, pressure drop in feed and permeate channels were neglected and linear approximation for concentration polarization term $e^{Jv/k}$ was assumed. Gupta et al., [12] have developed analytical design equations by neglecting pressure drops and assuming the mass transfer coefficient k to be a constant throughout the channel length. Further, the membrane was assumed to be a high rejection membrane. Ignoring the pressure drop in both channels as well as the increase in feed concentrations along the membrane, F. Evangelista and G. Jonsson [13] and F. Evangelista [14] have developed explicit analytical equations for water flux and tested these equations for dilute solutions. All these analytical solutions mentioned above are based on assumptions of average and uniform fluid conditions in feed and permeate channels. S. Avlontis et al., [15,16] have proposed an analytical solution for the spiral wound RO modules, which is the only analytical model reported in the literature that accounts for spatial variations in pressure, velocity and concentration in both the feed and permeate channels. This analytical model assumes constant value for mass transfer coefficient along the membrane and a linear approximation for the concentration polarization term $e^{Jv/k}$.

A number of rigorous models requiring numerical solutions are proposed in the literature [17,18] for spiral wound RO modules. M. Ben Bouldinar et al., [19] have developed a mathematical model taking into account the spatial variations of concentration, pressure and flow rates in feed and permeate channels and solved the model equations using finite difference methods. Evangelista and Johnson [18] have proposed a mathematical model using a three parameter model for membrane transport and developed a numerical procedure to solve the resulting nonlinear partial differential equations. Senthil Murugan et al. [20] have presented a model using Spiegler and Kedem model equations for membrane transport and solved the model equations by numerical method.

Any mathematical model can be regarded as reliable and practically significant only after it is validated with the experimental data. Also, validation of a mathematical model with the experimental data will lead to estimation of model parameters. Most of the model validation studies reported in the literature for spiral wound RO modules are primarily on validation of models with salt water desalination data. With an increasing trend in the application of spiral wound RO modules for treatment of waste water, studies on validation of mathematical models with experimental data on waste water contaminated with organic solutes gain importance. Not many investigations on validation of models with waste water data have been reported in the literature for spiral wound RO membrane modules.

This paper presents a new analytical model that yields explicit equations for spatial variations of pressure, fluid velocity and solute concentration on the feed channel side of the spiral wound RO module. As the fluid flow in the permeate side is much lower than the flow in the feed channel side, the pressure is assumed to be uniform in the permeate side. In this work, the mass transfer coefficient k is assumed to vary along the channel length of the module with varying fluid properties. Unlike the other analytical model reported by S. Avlontis et al., [15,16], the present work does not assume a linear approximation for concentration polarization term $e^{Jv/k}$. Further, the analytical equations derived in this paper are rearranged to give a new graphical method for the estimation of model parameters.

This paper series is written in two parts with the 'Theoretical Studies' covered in Part I and the 'Experimental Work' presented in Part II [1] of the paper. Development of analytical model equations and the graphical methods for estimation of model parameters are presented in Part I of the paper. In Part II [1], experimental studies on the removal of chlorophenol in a spiral wound RO module and the validation of model equations using the experimental data are reported.

2. Model development

A complete model for the spiral wound RO module is developed by combining the '*membrane transport equations*' that describe the solute and solvent flux through the membranes with the '*conservation and flow equations*' that describe the flow of material through the feed and the permeate channels of the module.

2.1. Membrane transport equations

The solution–diffusion model [21] is assumed to be valid for the transport of solvent and solute through the membrane. According to this model, solvent flux J_v and solute flux J_s through the membrane are expressed by the following equations

$$J_V = A_W(\Delta P - \Delta\Pi) \tag{1}$$

$$J_S = B_S(C_b - C_p) \tag{2}$$

where A_W is the solvent transport coefficient, B_S is the solute transport coefficient. The transmembrane pressure ΔP, which is the difference in pressures across the membrane, is defined as

$$\Delta P = (P_b - P_P) \tag{3}$$

where P_b and P_p are the pressures on the retentate side and permeate side of the membrane respectively. The osmotic pressure difference $\Delta\pi$ across the membrane is given by the Vant hoff's relation as

$$\Delta\Pi = \gamma T(C_b - C_p) \tag{4}$$

where γ is the gas law constant, T is the temperature, C_b and C_p are solute concentrations on the retentate side and permeate side of the membrane respectively. As the volumetric flux of solute is much lower than the volumetric flux of solvent, the following equation holds good

$$J_S = J_v \cdot C_p. \tag{5}$$

Concentration polarization [22] is the phenomenon in which the solute gets accumulated on the surface of the membrane causing substantial reduction in the rejection coefficient of the membrane. Accounting for the effect of concentration polarization, the concentration of solute at the membrane wall C_W is related to the bulk solute concentration C_b on the retentate side and the solute concentration C_p on the permeate side by the following relationship

$$\frac{C_W - C_p}{C_b - C_p} = e^{\left(\frac{J_v}{k}\right)} \tag{6}$$

where k is the mass transfer coefficient that characterizes the diffusive transport of solute through the boundary layer adjacent to the membrane. Taking the effect of concentration polarization, the equations for $\Delta\Pi$ and J_s are written in terms of C_W as follows

$$\Delta\Pi = \gamma T(C_W - C_p) \tag{7}$$

$$J_S = B_S(C_W - C_p). \tag{8}$$

Substituting Eq. (7) for $\Delta\Pi$ in Eq. (1), we get

$$J_v = A_W[\Delta P - \gamma T(C_W - C_p)]. \tag{9}$$

Substituting Eq. (8) for $(C_W - C_p)$ in Eq. (9), we get

$$J_v = A_W\left[\Delta P - \frac{\gamma T}{B_S} J_S\right]. \tag{10}$$

Writing J_s as the product of J_v and C_p, Eq. (10) is written as

$$J_v = A_W[\Delta P - \frac{\gamma}{B_S} TC_p J_v]. \quad (11)$$

Rearranging the above equation, the solvent flux J_v is written as

$$J_v = \frac{A_W \cdot \Delta P}{1 + \left(\frac{A_W \gamma}{B_S}\right) TC_p}. \quad (12)$$

The preceding equation shows that the solvent flux J_v through the membrane at any position depends only on the values of transmembrane pressure ΔP and permeate concentration C_p. Although the effect of concentration polarization on the solvent flux is not expressed explicitly in this equation, its effect is implicit in the calculation of C_p value using Eq. (13) given below

$$C_p = \frac{C_b}{\left[1 + \frac{J_v/B_S}{e^{J_v/k}}\right]}. \quad (13)$$

The preceding equation is derived by combining the Eqs. (6), (8) and (5).

2.2. Conservation and flow equations

The variation of fluid properties (flow, pressure and solute concentration) from one end of the module to the other end is described by writing the conservation and flow equations across the feed and permeate channels of the whole module. An appropriate description of the module geometry and dimensions is necessary to define the spatial coordinates for the conservation equations. A spiral wound module of length 'L' and diameter 'D' has a rectangular piece of membrane wound into 'n' number of turns. When the membrane in the spiral wound module is unwound, it assumes the shape of a rectangular piece shown in Fig. 1.

On one side of the membrane is the feed channel of thickness t_f and on the other side is the permeate channel of thickness t_p. Feed solution enters one end of the feed channel and comes out of the other end as reject solution. The solvent and the solute permeate through the membrane and gets collected in the permeate channel. One end of the permeate channel is sealed and through the other end which is open, the permeate flows out into a central duct. The flow of fluid is along the X-coordinate in the feed channel and along the Y-coordinate in the permeate channel.

The width of the feed channel 'W' is calculated using the equation

$$W = 2\pi\left(nD - n(n-1)\left(t_f + t_p\right)\right). \quad (14)$$

The cross-sectional areas of feed channel A_f and permeate channel A_p are

$$A_f = t_f W \quad (15)$$

$$A_p = t_p L \quad (16)$$

and the membrane area A_m is

$$A_m = L \cdot W. \quad (17)$$

The following assumptions are made regarding the spatial variations of flow, solute concentration and pressure in the feed and permeate channels.

1. No gradients of fluid velocity, solute concentration and pressure exist in the Z direction.
2. On the feed channel side, the fluid velocity u, fluid pressure P_b and the solute concentration C_b vary only in the direction of fluid flow, i.e. only in X direction and not in Y direction

$$\text{At } x = 0, \quad u(x) = \frac{F_i}{A_f}, \qquad P_b(x) = P_i, \quad C_b(x) = C_i \quad (18)$$

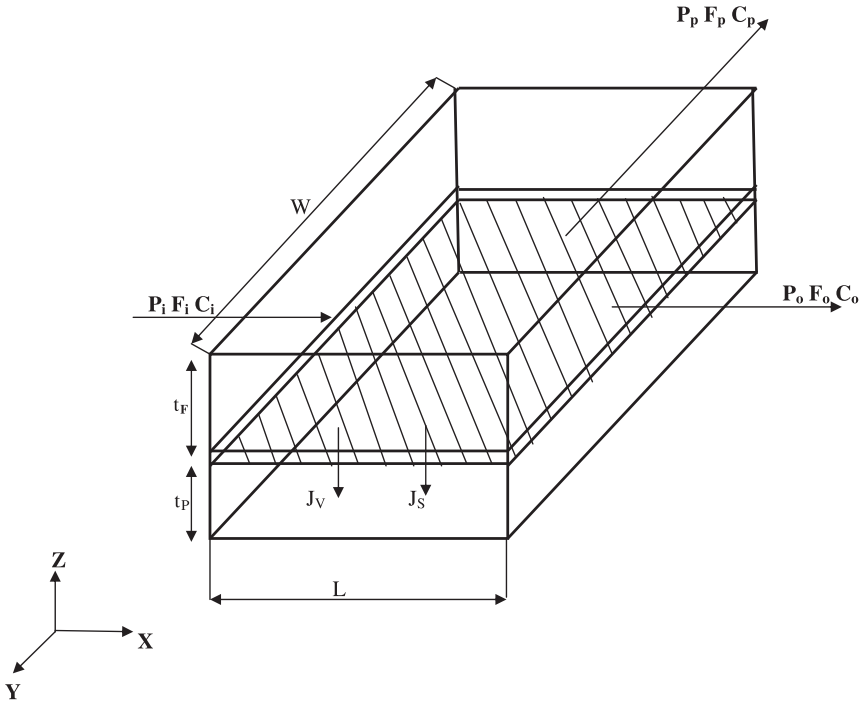

Fig. 1. Unwound configuration of spiral wound reverse osmosis membrane.

$$\text{At } x = L, \quad u(x) = \frac{F_o}{A_f}, \qquad P_b(x) = P_o, \qquad C_b(x) = C_o. \tag{19}$$

Here F_i, P_i and C_i are respectively the volumetric flow rate, pressure and solute concentration at the feed channel inlet and F_o, P_o and C_o are respectively the volumetric flow rate, pressure and solute concentration at the feed channel outlet.

3. As flow in the permeate channel is much lower than the flow in the feed channel, the pressure drop in the permeate channel is neglected leading to the assumption of uniform pressure P_p in the permeate channel.
4. On the permeate side, the fluid velocity u_p and permeate concentration C_p are assumed to vary along the spatial coordinates X and Y. As the permeate channel is sealed at one end ($y = 0$)

$$At\ y = 0, \quad u_p(x,y) = 0. \tag{20}$$

5. As the solution–diffusion model is assumed to be valid for the transport of solvent and solute through the membrane, the Eq. (12) derived for solvent flux J_v and the Eq. (5) for solute flux J_s are applicable at each and every location on the surface of the membrane. J_v and J_s also vary along X and Y co-ordinates as they are functions of transmembrane pressure ΔP and permeate concentration C_p.

Taking total mass balance and solute balance across a small section in the feed channel of the module, we get

$$\frac{du(x)}{dx} = -\frac{J_v}{t_f} \tag{21}$$

$$\frac{d}{dx}(u(x).C_b(x)) = -\frac{J_v}{t_f}C_p(x,y). \tag{22}$$

Similarly, total mass balance and solute balance across a small section in the permeate channel of the module gives

$$\frac{\partial u_p(x,y)}{\partial y} = \frac{J_v}{t_p} \tag{23}$$

$$\frac{\partial}{\partial y}(u_p(x,y).C_p(x,y)) = \frac{J_v}{t_p}C_p(x,y). \tag{24}$$

Applying product rule of differentiation, Eq. (24) can be written as

$$u_p(x,y).\frac{\partial}{\partial y}(C_p(x,y)) + C_p(x,y).\frac{\partial}{\partial y}u_p(x,y) = \frac{J_v}{t_p}.C_p(x,y). \tag{25}$$

Substituting Eq. (23) for $\frac{\partial u_p}{\partial y}(x,y)$ in Eq. (25), we have

$$\frac{\partial C_p(x,y)}{\partial y} = 0. \tag{26}$$

The preceding equation implies that C_p does not vary in Y direction and may be considered to vary only along X direction, i.e. $C_p(x,y) = C_p(x)$. This combined with the fact that the transmembrane pressure ΔP in Eq. (12) is only a function of x implies that the solvent flux J_v varies only in X direction and not in Y direction, i.e. $J_v(x,y) = J_v(x)$. Integrating Eq. (23) and taking $u_p(x,y) = 0$ at $y = 0$, we get

$$u_p(x,y) = \frac{J_v(x)}{t_p}y. \tag{27}$$

The volumetric flow rate of permeate $F_P(x)$ in the central permeate collection tube ($y = W$) at a distance x from the feed inlet is given by

$$F_p(x) = t_p\int_0^x u_p(x,W)dx. \tag{28}$$

Substituting Eq. (27) for $u_P(x,W)$ in Eq. (28), we get

$$F_p(x) = W\int_0^x J_v(x)dx. \tag{29}$$

The volumetric flow rate of fluid F(x) in the feed channel at a distance x from the feed inlet is

$$F(x) = A_f u(x). \tag{30}$$

Substituting Eq. (30) for u(x) in Eqs. (21) and (22) and taking $A_f = W\,t_f$, we have

$$\frac{dF(x)}{dx} = -W.J_v(x) \tag{31}$$

$$\frac{d}{dx}(F(x).C_b(x)) = -WJ_v(x).C_p(x). \tag{32}$$

Combining Eq. (31) and (32), we get

$$\frac{d}{dx}(F(x).C_b(x)) = C_p(x)\frac{dF(x)}{dx}. \tag{33}$$

Taking total mass balance and solute balance between the feed inlet position ($x = 0$) and a position at distance x from the inlet of the module, we have

$$F_i = F(x) + F_p(x) \tag{34}$$

$$F_i.C_i = F(x).C_b(x) + F_p(x).C_p(x). \tag{35}$$

Taking derivatives with respect to x on both sides of the Eqs. (34) and (35), we get

$$\frac{dF(x)}{dx} = -\frac{dF_p(x)}{dx} \tag{36}$$

$$\frac{d}{dx}(F(x).C_b(x)) = -\frac{d}{dx}(F_p(x).C_p(x)). \tag{37}$$

Combining Eqs. (33), (36) and (37) and applying product rule of differentiation, we get

$$\frac{d}{dx}(C_p(x)) = 0. \tag{38}$$

The preceding equation implies that the permeate concentration C_p does not vary in Y direction either. So the solute concentration is uniform in the permeate channel and can be taken as a constant. Although we assumed initially the permeate concentration to be varying in both X and Y directions, we have actually shown by solving the balance equations that the C_p value is indeed uniform in the permeate channel. This is as a result of assuming uniform pressure P_p in the permeate side. With C_p and P_p taking constant values in the permeate channel and the values of C_b, P_b and F varying along X direction in the feed channel, the spiral wound RO module can be schematically represented by a simplified diagram shown in Fig. 2.

Taking Eq. (12) to be applicable at every position on the surface of the membrane, The solvent flux J_v (x) through the membrane at a distance x from the feed channel inlet is proportional to the local transmembrane pressure $\Delta P(x)$

$$J_v(x) = \frac{A_W.\Delta P(x)}{1 + \left(\frac{A_W\gamma}{B_s}\right)TC_p} \tag{39}$$

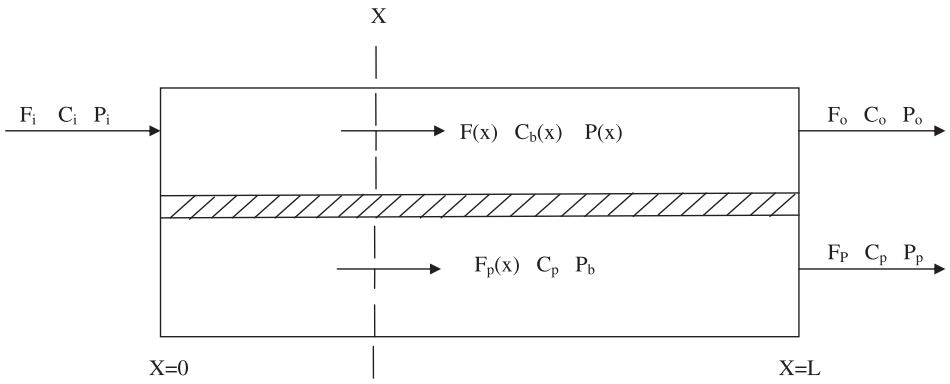

Fig. 2. Schematic representation of spiral wound reverse osmosis membrane module depicting spatial variations.

and transmembrane pressure ΔP(x) is

$$\Delta P(x) = P_b(x) - P_p \tag{40}$$

where $P_b(x)$ is the fluid pressure on the feed channel side at a distance x from the inlet. As the fluid flows through the feed channel, its pressure reduces from P_i at inlet to P_o at outlet. This pressure loss in the feed channel is due to wall friction as well as due to the drag caused by flow past internals. Assuming the Darcy's law to be applicable, the pressure gradient $\frac{dp_b(x)}{dx}$ in the feed channel at a distance x from the inlet is proportional to the volumetric flow rate F(x)

$$\frac{dp_b(x)}{dx} = -bF(x) \tag{41}$$

where the proportionality constant b is the feed channel friction parameter, which is determined experimentally.

Taking derivative with respect to x on both sides of Eq. (31),

$$\frac{d^2F(x)}{dx^2} = -W\frac{dJ_v(x)}{dx}. \tag{42}$$

Taking derivative of $J_v(x)$ with respect to x in Eq. (39) and combining it with Eq. (40), we have

$$\frac{dJ_v(x)}{dx} = \frac{A_W \cdot}{1 + \left(\frac{A_W \gamma}{B_s}\right) TC_p}\frac{dP_b(x)}{dx}. \tag{43}$$

Substituting Eq. (43) for $\frac{dJ_v(x)}{dx}$ in Eq. (42) and combining it with Eq. (41), we get

$$\frac{d^2F(x)}{dx^2} = \left[\frac{WbA_w}{(1 + A_w(\frac{\gamma}{B_s})TC_p)}\right]F(x) \tag{44}$$

Defining a dimensionless term ∅ as

$$\emptyset = L\sqrt{\frac{WbA_w}{(1 + A_w(\frac{\gamma}{B_s})TC_p)}} \tag{45}$$

and writing the Eq. (44) in terms of this dimensionless term, we have

$$\frac{d^2F(x)}{dx^2} = \frac{\emptyset^2}{L^2}F(x). \tag{46}$$

The preceding second order differential equation, with the boundary conditions for fluid flow rates defined at feed channel inlet and outlet,

$$\text{at } x = 0, F(x) = F_i \tag{47}$$

$$\text{at } x = L, F(x) = F_o \tag{48}$$

is solved to obtain an explicit analytical equation to calculate the feed channel fluid flow rate F(x) at a distance x from the feed inlet

$$F(x) = \frac{F_o \sinh\frac{\emptyset x}{L} + F_i \sinh\emptyset\left(1 - \frac{x}{L}\right)}{\sinh\emptyset}. \tag{49}$$

Rearranging the Equation (31) and writing the solvent flux $J_v(x)$ as a function of gradient of flow rate $\frac{dF(x)}{dx}$,

$$J_v(x) = -\frac{1}{W}\frac{dF(x)}{dx} \tag{50}$$

and substituting in this equation the derivative with respect to x of F(x), we obtain an equation for solute flux $J_v(x)$

$$J_v(x) = \frac{\emptyset}{A_m \sinh\emptyset}\left[F_i \cosh\emptyset\left(1 - \frac{x}{L}\right) - F_o \cosh\frac{\emptyset x}{L}\right]. \tag{51}$$

Substituting the preceding equation for $J_v(x)$ in Eq. (29), an expression for F(x) is obtained

$$F(x) = F_i - \frac{1}{\sinh\emptyset}\left[F_i \sinh\emptyset\left(1 - \frac{x}{L}\right) + F_o \sinh\frac{\emptyset x}{L}\right]. \tag{52}$$

Substituting F(x) from Eq. (49) in Eq. (41), we get an equation for pressure gradient

$$\frac{dP_b(x)}{dx} = \frac{-b}{\sinh\emptyset}\left[F_o \sinh\frac{\emptyset x}{L} + F_i \sinh\emptyset\left(1 - \frac{x}{L}\right)\right] \tag{53}$$

which on integration yields an expression for pressure profile $P_b(x)$

$$P_b(x) = P_i - \frac{bL}{\emptyset \sinh\emptyset}\left[F_o\left(\cosh\frac{\emptyset x}{L} - 1\right) - F_i\left(\cosh\emptyset\left(1 - \frac{x}{L}\right) - \cosh\emptyset\right)\right]. \tag{54}$$

Substituting in the above equation, the boundary condition for pressure at the feed channel outlet

$$\text{at } x = L, P_b(x) = P_o \tag{55}$$

an expression for the outlet pressure P_o is obtained

$$P_o = P_i - \frac{bL}{\emptyset \sinh\emptyset}\left[(F_i + F_o)(\cosh\emptyset - 1)\right]. \tag{56}$$

Introducing the dimensionless parameter ϕ in Eq. (39), the equation for $J_v(x)$ is written as

$$J_v(x) = \frac{\emptyset^2}{L^2 bW}\Delta P \tag{57}$$

where

$$\Delta P = P_b(x) - P_p. \tag{58}$$

Substituting in Eq. (57), $J_v(x)$ from Eq. (51) and $P_b(x)$ from Eq. (54), we get

$$\Delta P_i = \frac{bL}{\emptyset \sinh\emptyset}(F_i \cosh\emptyset - F_o) \tag{59}$$

where

$$\Delta P_i = P_i - P_p. \tag{60}$$

An expression for solute concentration $C_b(x)$ in the feed channel is derived by solving the balance Eq. (34) and (35).

$$C_b(x) = C_p + \frac{F_i(C_i - C_p)}{F(x)} \tag{61}$$

In this section, analytical equations have been derived to calculate the profiles of Flow F(x) (Eq. (49)), Solvent flux $J_v(x)$ (Eq. (51)), Pressure $P_b(x)$ (Eq. (54)) and Solute concentration $C_b(x)$ (Eq. (61)) in the feed channel of the spiral wound RO module. All these equations are functions of dimensionless parameter $\emptyset$ (Eq. (45)), which in turn is a function of permeate concentration C_p. The value of C_p is strongly influenced by concentration polarization whose effect is characterized by mass transfer coefficient 'k' as shown in the equation given below

$$C_p = \frac{C_b(x)}{\left[1 + \frac{J_v(x)/B_s}{e^{J_v(x)/k}}\right]}. \tag{62}$$

The preceding equation is rearranged to get an expression for the mass transfer coefficient k

$$k = \frac{J_v(x)}{\ln\left[\frac{J_v(x)}{B_s}\left(\frac{C_p}{C_{b(x)} - C_p}\right)\right]}. \tag{63}$$

It is evident from this equation that the mass transfer coefficient k varies along the feed channel length with varying conditions of fluid pressure, flow and solute concentration.

3. Estimation of model parameters

Reliability of any mathematical model in predicting the system behavior depends largely on accuracy of the values of model parameters. Appropriate estimation of parameter values is crucial for the effective use of a mathematical model as an analytical tool. Parameters of any model are usually estimated by matching the experimental data with model predictions. This is done either by using a rigorous least square optimization technique or by a graphical method of linear fit. The graphical method of parameter estimation is possible only if the model equations can be expressed in the form of a linear fit. As the model equations for the spiral wound RO module are solved and written in an analytical form, an attempt has been made in this work to develop graphical procedures for the estimation of model parameters.

The analytical model developed in the preceding section (Section 2) for the spiral wound RO modules has four parameters namely solvent transport coefficient A_W, solute transport coefficient B_S, mass transfer coefficient k and the feed channel fluid friction parameter b. The parameters A_W and B_S that characterize the transport of solvent and solute through the membranes are intrinsic properties of the membrane material and solvent and solute molecules. The parameter b that accounts for pressure loss due to friction in the feed channel depends on module dimensions and geometry. Graphical methods are developed in this work for the estimation of these three parameters A_W, B_S and b.

Unlike these three parameters, the other parameter namely the mass transfer coefficient k is strongly influenced by operating conditions such as flow. The mass transfer coefficient k characterizes the transfer of solutes in the concentration polarization layer of RO membranes. Usually, k is estimated using standard correlations [23,24] for mass transfer coefficient reported for flow through tubes. A method for estimation of k from the experimental data is presented in this work.

Experimental data required for estimation of model parameters are generally obtained by conducting suitable experiments on a spiral wound RO module with solutions containing a specific chemical compound. In these experiments, the operating parameters namely feed flow F_i, feed pressure P_i and feed concentration C_i are varied over a range of values and the readings of reject flow F_o, reject concentration C_o, outlet pressure P_o and permeate concentration C_p are recorded. In the part II of this paper series, details of the experimental studies carried out will be reported.

3.1. Estimation of parameters A_W, B_S and b

A graphical procedure for the estimation of parameters A_W, B_S and b is developed in this section by deriving necessary equations. The pressure drop $(P_i - P_o)$ on the feed channel side derived from Eq. (56) is

$$P_i - P_o = \frac{bL}{\emptyset \sinh\emptyset}[(F_i + F_o)(\cosh\emptyset - 1)] \tag{64}$$

The transmembrane pressure $(P_i - P_p)$ at the feed inlet derived from Eq. (59) is

$$P_i - P_p = \frac{bL}{\emptyset \sinh\emptyset}(F_i \cosh\emptyset - F_o). \tag{65}$$

Define a dimensionless term β as the ratio of pressure drop $(P_i - P_o)$ on the feed channel side to the transmembrane pressure $(P_i - P_p)$ at the feed inlet

$$\beta - \frac{P_i - P_o}{P_i - P_p}. \tag{66}$$

Combining Eqs. (64), (65) and (66), we have

$$\beta = \frac{(F_i + F_o)\cdot(\cosh\emptyset - 1)}{F_i \cosh\emptyset - F_o}. \tag{67}$$

Rearranging the preceding equation, we get an expression for the calculation of dimensionless parameter $\emptyset$ as a function of measured readings of F_i, F_o, P_i and P_o

$$\emptyset = \cosh^{-1}\left[\frac{(F_i + F_o)\beta . F_o}{(F_i + F_o)\beta F_i}\right]. \tag{68}$$

Taking the definition of ∅ given in Eq. (45) and rearranging the terms in this equation, we get

$$\frac{1}{\emptyset^2}\left(\frac{\gamma}{L^2WbB_s}\right)TC_p + \frac{1}{(L^2WbA_w)}. \tag{69}$$

This equation represents a straight line fit on the plot of $\frac{1}{\emptyset^2}$ vs T C_p (Fig. 3) with slope S_1 and Intercept I_1.

$$S_1 = \left(\frac{\gamma}{L^2WbB_s}\right) \tag{70}$$

$$I_l = \left(\frac{1}{L^2WbA_w}\right). \tag{71}$$

Similarly, it is implied from Eq. (64) that a plot of $(P_i - P_o)$ vs . $\frac{L}{\emptyset \sinh\emptyset}\left[(F_i + F_o)(\cosh\emptyset - 1)\right]$ (Fig. 4) is a straight line passing through origin with slope S_2 equal to b

$$S_2 = b. \tag{72}$$

These two plots shown in Figs. 3 and 4 are drawn using the experimental readings of F_i, F_o, P_i, P_o, T and C_p. The slopes and intercepts S_1, I_1 and S_2 of the best linear fits matching the experimental data points are calculated by the method of least squares. The values of parameters A_W, B_S and b are estimated by solving the Eq. (70), (71) and (72). Details of experimental studies and the estimation of values of A_W, B_S and b using the experimental data are reported in Part II of this paper series [1].

3.2. Estimation of mass transfer coefficient, k

The parameter k is the mass transfer coefficient, which is usually estimated using standard correlations reported for estimation of mass transfer coefficients for flow through tubes or rectangular channels [23–27]. The correlations used for the estimation of k are of the standard form

$$Sh = p\,Re^q Sc^r \tag{73}$$

where Sh is the Sherwood number ($Sh = kd_e/D_A$), Re is the Reynolds number ($Re = d_e u\rho/\mu$) and Sc is the Schmidt number ($Sc = \mu/\rho D_A$). These correlations establish the dependence of mass transfer coefficient on the fluid dynamics and solute/solvent characteristics. Correlations of this form are generally used for calculation of k in concentration polarization layers of RO membranes. Critical reviews have been reported [23] on the factors that need to be considered in adapting the standard correlations for mass transfer in concentration polarization layers. Most of the reports [20,26,28] on validation of standard mass transfer correlations for RO membranes are confined to seawater desalination data and no report on validation of these correlations for solutes other than salt has been found in the literature.

Application of standard correlations for the estimation of mass transfer coefficients for RO membranes have been severely criticized [16,29,30]. According to standard correlations of the form represented by Eq. (73), the mass transfer coefficient k is essentially influenced by fluid velocity and solute/solvent properties. However, a number of experiments reported in the literature [15,16,31] show that factors like solvent flux, pressure and solute concentrations apart from fluid velocity and solute/solvent properties also affect mass transfer coefficient k. In any convective mass transfer process, the mass transfer takes place by diffusion of solutes in boundary layer, while in membrane process, solute transport in concentration polarization layer occurs not only by convection but also by advection. The effect of advection on concentration polarization can at times be more significant than diffusion. The standard correlations account only for the effect of diffusive transport of solute on mass transfer coefficient but fail to take into consideration the effect of advective transport. When the advective transport of solutes is also taken into account, the actual mass transfer coefficient k, unlike the one estimated using standard correlations, could possibly be influenced by a number of factors in addition to fluid velocity and solute/solvent properties [32].

An attempt is made in this work to establish from experimental data if the mass transfer coefficient k is influenced by factors other than fluid velocity, solute and solvent properties. Hence, the method developed here for estimation of mass transfer coefficient assumes the value of k to be varying from one end of the module to the other end with varying conditions of fluid velocity, pressure and solute concentration along the feed channel length. Rewriting the Eq. (63), the mass transfer coefficient at a distance x from the feed inlet is given by

$$k_{(x)} = \frac{J_v(x)}{\ln\left[\frac{J_v(x)}{B_S}\left(\frac{C_p}{C_b(x)^{-C_p}}\right)\right]}. \tag{74}$$

As the conditions of flow, pressure and solute concentration at the inlet (x = 0) and outlet (x = L) ends of the module are measured, the values of mass transfer coefficients at these two ends of the module are estimated using these measured data.

At module inlet (x = 0), the mass transfer coefficient k_i is

$$k_i = \frac{J_v(0)}{\ln\left[\frac{J_v(0)}{B_S}\left(\frac{C_p}{C_i - C_p}\right)\right]} \tag{75}$$

where

$$J_v(0) = \frac{A_W.\Delta P_i}{1 + \left(\frac{A_W\gamma}{B_S}\right)TC_p} \tag{76}$$

$$\Delta P_i = P_i - P_p. \tag{77}$$

At module outlet (x = L), the mass transfer coefficient k_o is

$$k_o = \frac{J_v(L)}{\ln\left[\frac{J_v(L)}{B_S}\left(\frac{C_p}{C_o - C_p}\right)\right]} \tag{78}$$

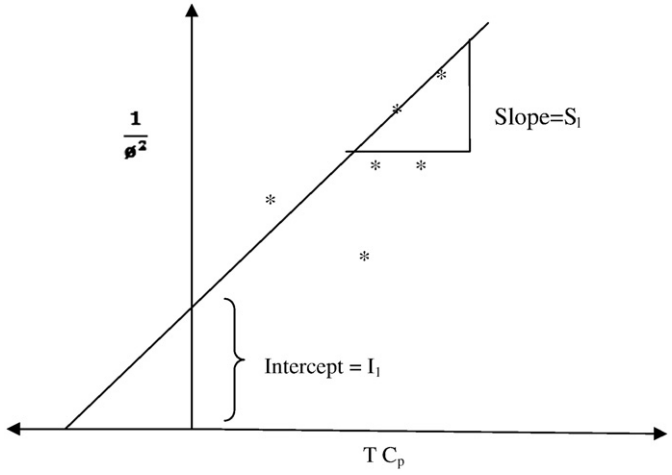

Fig. 3. Plot of $\frac{1}{\emptyset^2}$ vs TC_p for estimation of A_w and B_s.

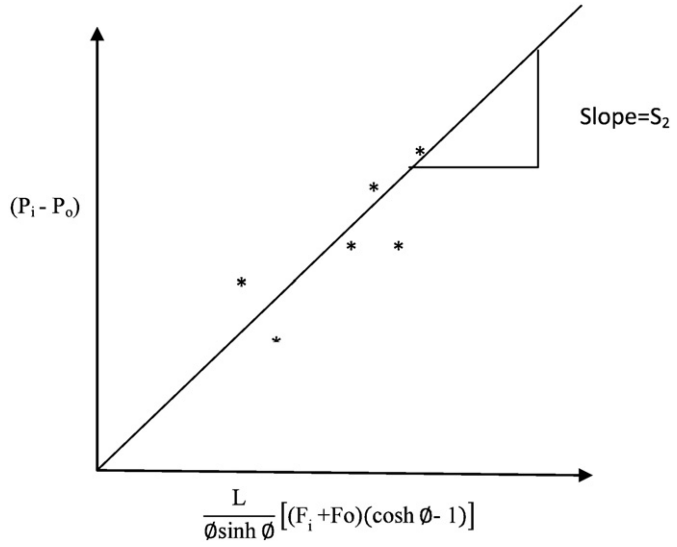

Fig. 4. Plot of $(P_i - P_o)$ vs $\frac{L}{\emptyset\, sinh}\emptyset[(F_i + F_o)(\, cosh\,\emptyset - 1)]$ for estimation of b.

where

$$J_v(L) = \frac{A_W \cdot \Delta P_o}{1 + (\frac{A_W \gamma}{B_S})TC_p} \tag{79}$$

$$\Delta P_o = P_o - P_p. \tag{80}$$

The mass transfer coefficients are estimated at the inlet and outlet ends of the spiral wound RO module by making use of the estimated values of membrane transport parameters A_W, B_S and experimental readings of P_i, C_i, F_i, P_o, C_o, F_o, T and Cp in Eqs. (75)–(80). A correlation analysis of the estimated values of k will establish the influence of various factors on mass transfer coefficient. The experimental studies and the estimation of mass transfer coefficient are reported in Part II of this paper series [1].

4. Conclusions

A mathematical model was developed for spiral wound RO module assuming spatial variations of pressure, flow rate, and solute concentration in the feed channel and uniform condition of pressure in the permeate channel. Validity of the solution–diffusion model with concentration polarization was assumed for transport of solvent and solute through the membrane. As a result of these assumptions, it was shown in this work that the permeate concentration C_p would assume a uniform value in the permeate channel (Eq. (38)). Explicit analytical equations were derived for prediction of spatial variations of pressure, flow rate, solvent flux and solute concentration in the feed channel.

The model has four parameters namely solvent transport coefficient A_W, solute transport coefficient B_S, feed channel friction parameter b and the mass transfer coefficient k. Procedures for estimation of these model parameters were presented in this work. Explicit equations were derived for estimation of parameters A_W, B_S and b by the method of linear graphical fit. The mass transfer coefficient k is assumed to vary from one end to the other end of the module with varying conditions of flow, pressure and solute concentration in the feed channel. Explicit equations for the estimation of k were derived.

Theoretical studies on the development of mathematical model and the methods for estimation of model parameters are presented in Part I of this paper and in the continuation of this paper series in Part II [1], the experimental work on the validation of the mathematical model and estimation of model parameters are presented.

Symbols

A_f	feed channel area (m^2)
A_m	membrane area (m^2)
A_p	permeate channel area (m^2)
A_w	solvent transport coefficient (m/atm·s)
b	feed channel friction parameter (atm·s/m^4)
B_s	solute transport coefficient(m/s)
C_b	concentration of solute in the feed channel (kmole/m^3)
C_i	concentration of solute in the feed (kmole/m^3)
C_o	concentration of solute in the retentate (kmole/m^3)
C_p	concentration of solute in the permeate (kmole/m^3)
C_w	concentration of solute at the membrane wall (kmole/m^3)
F_i	feed flow rate (m^3/s)
F_p	permeate flow rate (m^3/s)
F_o	retentate flow rate (m^3/s)
J_s	solute flux (kmole of solute/m^2 s)
J_v	solvent flux (m/s)
k	mass transfer coefficient (m/s)
k_i	mass transfer coefficient at the inlet (m/s)
k_o	mass transfer coefficient at the outlet (m/s)
L	RO module length (m)
D	module diameter(m)
D_A	diffusivity (m^2/s)
d_e	equivalent diameter of feed channel (m)
n	number of turns in the spiral wound module
P_b	pressure in the feed channel (atm)
P_i	PRESSURE at the feed channel inlet (atm)
P_o	pressure at the feed channel outlet (atm)
P_p	pressure in the permeate channel (atm)
p	coefficient appearing in Eq. (73)
q	exponent of Reynolds number appearing in Eq. (73)
r	exponent of Schmidt number appearing in Eq. (73)
Re	Reynolds number
Sh	Sherwood number
Sc	Schmidt number
t_f	feed spacer thickness, m
t_P	permeate channel thickness, m

T	temperature (K)
u	fluid velocity in feed channel (m/s)
u_p	fluid velocity in permeate channel (m/s)
W	RO module width (m)
x	axial position in feed channel
y	axial position in permeate channel
X, Y,Z	Cartesian co-ordinates

Greek symbols

β	a dimensionless parameter, defined in Eq. (66)
Δ	difference across the membrane
ΔP	transmembrane pressure(atm)
$\Delta\ \Pi$	difference in osmotic pressures across the membrane (atm)
ϕ	dimensionless term defined in Eq. (45)
γ	gas law constant $\left(\gamma = R, 0.0820 \frac{atm\, m^3}{^oK kmol}\right)$
μ	viscosity (kg/ms)
Π	osmotic pressure (atm)
ρ	density (kg/m^3)

References

[1] S. Sundaramoorthy, G. Srinivasan, D.V.R. Murthy, 'An analytical model for spiral wound reverse osmosis membrane modules : Part-II — Experimental validation', Desalination 277 (1–3) (2011) 257–264.
[2] A. Bodalo-Santoyo, J.L. Gomez-Carasco, E. Gomez-Gomez, M.L. Maximo-Martin, A.M. Hidalgo-Montesinos, Application of reverse membrane to reduce pollutants present in industrial waste water, Desalination 155 (2003) 101–108.
[3] W. Guo, R. Zhang, S. Vigneswaran, H. Ngo, J.K. Kandasamy, Membranes coupled with physico chemical treatment in water reuse, Water Sci. Technol. 61 (2010) 513–519.
[4] T. Nguyen, S. Vigneswaran, H. Ngo, H. Shon, J.K. Kandasamy, Arsenic removal by a membrane hybrid filtration system, Desalination 236 (2009) 363–369.
[5] C.S. Slater, R.C. Ahlert, C.G. Uchrin, Applications of Reverse Osmosis to complex industrial wastewater treatment, Desalination 48 (1983) 171–187.
[6] Y. Yoon, R.M. Lueptow, Removal of organic contaminants by RO and NF membranes, J. Membr. Sci. 261 (1–2) (2005) 76–86.
[7] A. Allegrezza, Commercial Reverse Osmosis membranes and modules, in: B. Parekh (Ed.), Reverse Osmosis Technology, Marcel Dekker, Inc., New York, 1988, pp. 53–120.
[8] D. Bhattacharyya, M. Williams, Introduction and definitions — Reverse Osmosis, in: W. Ho, K. Sirkar (Eds.), Membrane Handbook, Van Nostrand Reinhold, New York, 1992, pp. 265–268.
[9] D. Bhattacharyya, M. Williams, Theory — Reverse Osmosis, in: W. Ho, K. Sirkar (Eds.), Membrane Handbook, Van Nostrand Reinhold, New York, 1992, pp. 269–280.
[10] J. Marriott, E. Sorensen, A general approach to modeling membrane modules, Chem. Eng. Sci. 58 (2003) 4975–4990.
[11] K.K. Sirkar, P.T. Dong, G.H. Rao, Approximate design equations for reverse osmosis desalination by spiral wound modules, Chem. Eng. Sci. 21 (1982) 517–527.
[12] S.K. Gupta, Analytical design equations for reverse osmosis systems, Ind. Eng. Chem. Process Des. Dev. 24 (1985) 1240.
[13] F. Evangelista, G. Jonsson, Optimum design and performance of spiral wound modules II: analytical method, Chem. Eng. Commun. 72 (1988) 83–94.
[14] F. Evangelista, A short cut method for the design of reverse osmosis desalination plants, Ind. Eng. Chem. Process Des. Dev. 24 (1985) 211–223.
[15] S. Avlonitis, W.T. Hanbury, M. Ben Boudinar, Spiral wound modules performance An analytical solution: Part I, Desalination 81 (1991) 191–208.
[16] S. Avlonitis, W.T. Hanbury, M. Ben Boudinar, Spiral wound modules performance an analytical solution: Part II, Desalination 89 (1993) 227–246.
[17] J.I. Marriott, E. Sorensen, I.D.L. Bogle, Detailed mathematical modeling of membrane modules, Comput. Chem. Eng. 25 (2001) 693–700.
[18] F. Evangelista, G. Jonsson, Optimum design and performance of spiral wound modules I: numerical method, Chem. Eng. Commun. 72 (1988) 69–81.
[19] M. Ben Boudinar, W.T. Hanbury, S. Avlonitis, Numerical simulation and optimisation of spiral-wound modules, Desalination 86 (1992) 273–290.
[20] S. Senthilmurugan, Aruj Ahluwalia and S.K. Gupta, Modeling of a Spiral-wound module and estimation of model parameters using numerical techniques, Desalination 173 (2005) 269–286.
[21] H. Lonsdale Test, Article sample title placed here, J. Membr. Sci. 51 (1990) 1–81.
[22] C.E. Boesen, G. Jonsson, Polarization phenomena in membrane processes, in: G. Belfort (Ed.), Synthetic Membrane Processes, Academic Press, New York,NY, 1983, Ch.4.
[23] V. Gekas, B. Hallstrom, Mass transfer in the membrane concentration polarization layer under turbulent cross flow.I, Critical literature review and prediction of existing Sherwood correlations to membrane operations, J. Membr. Sci. 30 (1987) 153.
[24] P.C. Wankat, Rate-controlled Separations, Springer International, 1994.
[25] G. Schock, A. Miquel, Mass transfer and pressure loss in spiral wound modules, Desalination 64 (1987) 339–352.
[26] Z.V.P. Murthy, Sharad K. Gupta, Estimation of mass transfer coefficient using a combined nonlinear membrane transport and film theory model, Desalination 109 (1997) 39–49.
[27] A. Chiolle, G. Gianotti, M. Gramondo, G. Parrini, Mathematical model of reverse osmosis in parallel–wall channels with turbulence promoting nets, Desalination 26 (1978) 3.
[28] Y. Taniguchi, An analysis of reverse osmosis characteristics of ROGA spiral-wound modules, Desalination 25 (1978) 71.
[29] G. Belfort, N. Negata, Fluid mechanics and cross-filtration filtration: some thoughts, Desalination 53 (1985) 57.
[30] G. Jonsson, Boundary layer phenomenon during ultrafiltration of dextran and whey protein solutions, Desalination 51 (1984) 61.
[31] P. Erikson, Water and Salt transport through two types of polyamide composite membranes, J. Membr. Sci. 36 (1988) 297–313.
[32] V. Geraldes, V. Semilao, M.N. Pinho, Flow and mass transfer modelling of nanofiltration, J. Membr. Sci. 191 (2001) 109–128.